Experimental Validation of Neural-Network-Based Nonlinear Reduced-Order Model for Vertical Sloshing

Marco Pizzoli*, Francesco Saltari†, Giuliano Coppotelli‡, Franco Mastroddi§
Dept. of Mechanical and Aerospace Engineering
Sapienza University of Rome
Via Eudossiana 18, 00184 Rome, Italy
franco.mastroddi@uniroma1.it

In this paper, a nonlinear reduced order model based on neural networks is introduced in order to model vertical sloshing for use in fluid-structure interaction simulations. A box partially filled with water, representative of a wing tank, is first tested to identify a neural network model and then attached to a cantilever beam to test the effectiveness of the neural network in predicting the sloshing forces when coupled with the structure. The experimental set-up is equipped with accelerometers and load cells at the interface between the tank and an electrodynamic shaker, which provides vertical acceleration to the tank. Accelerations and interface forces measured during the experimental tests are employed to identify a recurrent network able to return the vertical sloshing forces when the tank is set on vertical motion. The identified model is then experimentally tested and assessed by its integration on the tip of a cantilever beam. The free response of the experimental setup are compared with those obtained by simulating an equivalent virtual model in which the identified reduced-order model is integrated to account for the effects of vertical sloshing.

I. Introduction

The dissipative effects of a fluid inside commercial aircraft tanks have not specifically been looked at in the past to reduce the resulting dynamic loads. The identification and the study of such dynamic effects can make it possible in the future to design less conservative aircraft configurations, thus enabling increasingly lighter structures and, as a consequence, having a less polluting impact on the environment. In this paper, we experimentally identify the vertical sloshing, that mainly occurs on structures that undergo strong vertical accelerations. Aeronautical structures usually withstand loads occurring from gusts, turbulence and landing impacts. The sloshing of fuel generally stowed in the wing tanks caused by vertical accelerations is coupled with the structural dynamics of the aircraft by means of impacts between fluid propellant and tank walls. This type of sloshing is well known to provide a noticeable increase in the overall structural damping. This research activity is framed in the European project H2020 SLOshing Wing Dynamics (SLOWD) aiming with an heuristic approach (combining experimental and numerical data) at characterising sloshing dynamics for its use in future aircraft design (Ref. [1]).

Vertical slosh dynamics is one of the possible dynamics of the fluid stowed in the tanks which, when it occurs, exhibits different characteristics compared to the classic sloshing, generally occurring with rotations and lateral motions of the tank (see Refs. [2–5]). The latter motion generates standing waves inside the cavity that provide dynamic coupling with structure and possible modification of flutter margins. Specifically, the effects of sloshing on aircraft aeroelastic flutter stability was considered in Refs. [6–8]. On the other hand, the subject of this paper is sloshing induced by vertical acceleration of the tank, hence perpendicular to the free surface.

At very low excitation levels, the free surface tends to remain flat. By increasing the level of vertical acceleration some modes can become unstable depending on the oscillation frequency (Refs. [3, 9, 10]). Nonlinearities will generate fluid fingers that can reach the tank ceiling. By increasing the level of acceleration even more, presumably around $1g$, the transition to a completely chaotic regime takes place. Indeed, higher values of vertical acceleration trigger Rayleigh-Taylor instabilities (Ref. [9]), determining a chaotic flow regime with air/water mixing.

*PhD student.
†Research fellow.
‡Associate Professor.
§Full Professor.

Previous experimental fluid-structure interaction campaigns in which a tank system was positioned at the tip of a beam, representing a wing, showed how this type of chaotic response induces a very damped response of the structure (Refs. [11–14]). Indeed, turbulence, impacts and the continuous generation of the free surface cause additional dissipation of energy. The total balancing of elastic potential energy and fluid energy results in a noticeable increase in the effective damping of the structural motion. Moreover, for vertical harmonic motions, the dissipative characteristics depend on the frequency as well as on the amplitude of the motion (Ref. [15, 16]). As a consequence, vertical sloshing can not simply be described by means of linear viscoelastic models in which the loss of energy depends only on the oscillation frequency [17, 18], such as fractional derivatives and finite states for the damping (see Ref. [19]). Nonlinear predictive models are therefore necessary to simulate the impact the sloshing forces have on the dissipation of the elastic energy. An equivalent mechanical model consisting of a bouncing ball capable to reproduce the impact mechanisms, was proposed by Refs. [20, 21]). The proposed models provide fast prediction of sloshing forces, but they do not provide results that can generally be applied to frequencies different from those used in their training.

The aim of this work is to identify nonlinear vertical sloshing using a machine learning technique for nonlinear systems with a neural network that learns from data through a suitable training process. Refs. [22, 23] introduced the use of artificial neural network for real-time prediction of the sloshing loads in cargo containers. Considering the black box nature of the system under consideration, input-output data from high-fidelity numerical simulations (CFD) or experiments with varying frequencies and amplitudes are likely to be the most useful for implementing this technique.

In Ref. [15], an experimental campaign was carried out to characterise the dissipative behaviour of vertical sloshing as a function of excitation frequency and amplitude. The same setup is here employed to generate an experimental data set to train a recurrent neural network (Ref. [24]) for vertical sloshing. The identified network is then experimentally validated by performing a new experiment in which the tank used for identification is placed at the end of a cantilever beam. The comparison of the simulation of the beam free response with the analogous experimental result provide the assessment and validation of the approach.

Within the paper the following problems are defined: *i) Open-loop* problem consisting of experiment with a small box-shaped tank placed above the electrodynamics shaker to generate data from pseudo-harmonic test and the identification of the associated neural-network-based ROM by *training* process that employs the measurements; *ii) Closed-loop* problem consisting of the *sloshing beam* experiment in which the same tank is placed at the tip of a beam structure to perform a free response analysis and the analogous numerical model in which the identified neural-network-based ROM is integrated into the structural dynamics formulation.

The paper is organised as it follows. The sloshing beam problem, taken as an example of a general structure with sloshing tank inside, is introduced in Sec. II; the sloshing open-loop problem is presented in Sec. III whereas the closed-loop problem (sloshing beam response) is introduced in Sec. IV where the comparison between experimental and the numerical results is provided. A concluding remarks section ends the paper.

II. The sloshing beam problem

The object of this section is to mathematically introduce the problem of a cantilever beam with a sloshing liquid in a tank placed at its end, assumed perfectly symmetrical with respect to the vertical plane passing through the elastic centre and in which the displacement field is linear and purely vertical. The structural displacements $u(x,t)$ can be expressed by

$$u(x,t) \simeq \sum_{n=1}^{N} \psi_n(x) q_n(t) \tag{1}$$

where $\psi_n(x)$ are the modes of vibrations of the structure and $q_n(t)$ are the generalised coordinates describing the body deformation in time. Note that a space-discretization for the structure is assumed by including a finite number N of modes in the analysis, *i.e.,* a frequency-band-limited unsteady process. Considering this displacement representation for aircraft wing dynamics, one has the following Lagrange equations of motion in terms of N modal coordinates $q_n(t)$

$$\mathsf{M}\ddot{\mathsf{q}} + \mathsf{K}\mathsf{q} = \mathsf{g} + \mathsf{f}^{(ext)} \tag{2}$$

where $\mathsf{q} = [q_1, q_2, \ldots, q_N]^{\mathrm{T}}$ is the modal coordinates vector, $\mathsf{M} = \mathrm{diag}(m_1, m_2, \ldots m_N)$ and K are, respectively, the modal mass and stiffness (diagonal) matrices, whereas $\mathsf{g} = [g_1, g_2, \ldots, g_N]^{\mathrm{T}}$ is the vector of the generalised *sloshing* forces induced by the elastic motion. The $\mathsf{f}^{(ext)}$ is the vector of the current external forcing terms.

The *n-th* component of g is the projection of the pressure distribution p_S on each *n-th* modal shape ψ_n by integrating the inner product on the *i-th* tank wet surface $\mathcal{S}_{tank}$ as in the following ($\mathbf{n}$ unit normal vector to $\mathcal{S}_{tank}$ and $\mathbf{i}_3$ vertical

unit vector)

$$g_n = -\oiint_{\mathcal{S}_{tank}} p_S \ \mathbf{n} \cdot \mathbf{i}_3 \, \psi_n \, d\mathcal{S} \tag{3}$$

By assuming a rigid tank identified by its geometrical centre, Eq. 3 can be recast as:

$$g_n = f_S \, \psi_n(x_T) + m_S \, \varphi_n(x_T) \tag{4}$$

where f_S and m_S are, respectively, the sloshing force and moment applied in the geometric centre of the tank x_T, whereas $\varphi_n(x_T) = \mathrm{d}\psi_n/\mathrm{d}x(x_T)$ is the *n-th* modal rotation of the point x_T. A sloshing force is decomposed in this work by considering two contributions: the inertial force as for the frozen configuration and the perturbation caused by the relative motion of the fluid particles within the tank. Assuming there is only a vertical perturbation Δf_{S_z} and that the moment m_S about the geometric centre of the tank is negligible, the sloshing force f_S is given by:

$$f_S \quad = \quad -\sum_{k=1}^{N} m_l \, \psi_k(x_T) \, \ddot{q}_k + \Delta f_{S_z} \tag{5}$$

where $\mathbf{d}$ is the offset between the geometric centre of the tank and the liquid centre of mass and $\mathbf{I}_l$ is the inertia tensor of the frozen fluid. It is worth noting that Δf_{S_z} is a non-conservative force that is a nonlinear function of the history of the tank vertical displacement $u_z(x_T, t)$. By considering Eq. 5, Eq. 4 can be recast as:

$$g_n = m_l \, \psi_n(x_T) \, \psi_k(x_T) \, \ddot{q}_k + \psi_n(x_T) \, \Delta f_{S_z} \tag{6}$$

where Δm_{nk} is a component of the added mass given by the inertia of the fluid. Section III characterises Δf_{S_z} by its experimental data-driven identification using neural networks.

III. Sloshing open-loop problem

In this section, sloshing dynamics is treated as an isolated system that can be studied separately to shed light on its constitutive properties. Section III.A presents the experimental case study already used in Ref. [15] to characterise the dissipation caused by vertical sloshing. Section III.B describes how this experiment is used to generate high-fidelity data to identify a reduced-order model. Finally, Sec. III.C presents the training process of a reduced-order model based on a neural network.

A. Experimental test case of the isolated sloshing-tank

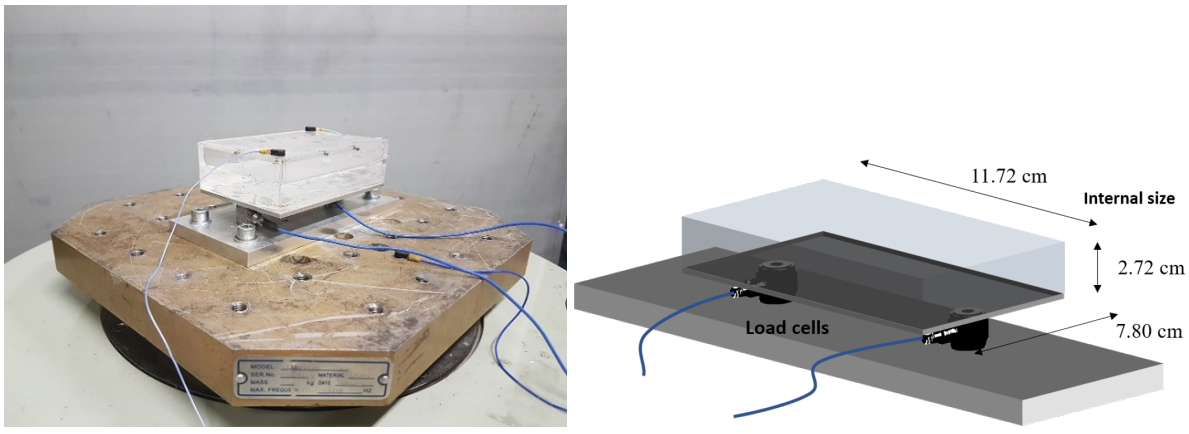

(a) Experimental Set-up (b) layout

Fig. 1 Experimental Configuration

The experimental case study is a small-box-shaped tank made in plexiglass placed over a controlled electrodynamic shaker, able to impose vertical sinusoidal displacement. The dimensions of the tank, a height of $h = 27.2$ mm and

the base of the sides $l_1 = 117.2$ mm and $l_2 = 78.0$ mm, are chosen so that the liquid collides with the roof of the tank, according to the maximum achievable limits of the shaker (25 mm peak-to-peak amplitude of displacement). The dynamic load at the interface between shaker and tank is measurable by two load cells (See Fig. 1), symmetrically placed along the mid-line of the long side of the tank base. The overall force exchanged by tank and shaker is the sum of the two load cells. The system is also equipped with two redundant accelerometers placed at the opposite corners of the tank upper closing side and with an accelerometer used by the shaker controller. This experimental set-up is the same one that was used in Ref. [15] to study the dissipative properties of fluid sloshing within a tank set in vertical motion. The quantification of the energy dissipated by the fluid was performed for different values of oscillation amplitudes and frequencies in order to characterise the sloshing nonlinear dissipative behaviour. These two parameters are strictly related to the unsteady boundary conditions that a vertically vibrating structure can impose to the walls of a tank that interfaces with it. The frequency and amplitude ranges considered covered both the region of small perturbations (low values of acceleration) where Faraday waves occur and the region corresponding to high accelerations where intense impacts between liquid and tank roof can occur after the fragmentation of the free surface (Rayleigh-Taylor instabilities). To better interpret the mechanisms of energy dissipation, the test design included an analysis at different filling levels (25 %, 50 % and 75 %).

Without any regard to the filling level, vertical sloshing provided always maximum dissipation beyond the 1 g of acceleration. The maximum relative dissipation seems to be linked to the oscillation amplitude values owe to a sort of spatial synchronisation of the movement of the fluid with that supplied to the tank. The processed results showed that the energy dissipated by the sloshing forces highly depends on the intensity of the excitation. More in details, a low dissipation level has been noted for acceleration values lower than a 1 g. The dissipated energy maps are not simply monotonically dependent on the amplitude levels of the vertical acceleration. Indeed, surface tension and viscosity seem to play a role in stabilising the free surface at higher frequency range even at acceleration values higher than 1 g. Moreover, beyond a certain level of acceleration (around $4g$) the dissipation mechanisms becomes less effective. This motivates the possibility of collecting data that will be used for identifying vertical sloshing forces only over a specific range of frequency.

B. Data collection for network training

The experimental setup presented in the previous section was used to generate a high-fidelity data set for training a neural network. To this end, an additional test was performed in conjunction with the previously presented experimental campaign: a very long pseudo-harmonic motion was assigned to the shaker (by considering the reference filling level corresponding to the 50 %). In this experimental test, the vertical sloshing is considered as an isolated system that receives as input a motion (or acceleration) imposed externally by the electromechanical shaker and returns as output a force (related to the relative motion of the liquid inside the tank and to possible impacts of the droplets against the tank walls). Figure 2(a) shows the path considered for the pseudo-harmonic test, plotted as a function of non-dimensional frequency and velocity (that, for the vertical slosh dynamics assumes the meaning of Froude number, see Refs.[16, 25]) which are respectively defined as $\bar{\omega} = \Omega/\sqrt{g/h}$ and $\bar{v} = v/\sqrt{gh}$ (where Ω is the excitation frequency and $a = v/\Omega$ is the amplitude of the vertical imposed motion). The acceleration assigned by the shaker, parametrized by time with the law $\ddot{u}_z = f(t)\cos(\int \Omega(t)\mathrm{d}t)$, was such as to suitably cover the non-dimensional amplitude and frequency domain of interest, that is highlighted in Fig. 2(b). In detail, the last figure shows the non-dimensional energy dissipated by the sloshing fluid $L_d/(m_l a^2\Omega^2)$ (with L_d the energy dissipated by the fluid per cycle and m_l the total mass of the fluid) in a vertical harmonic motion $u_z = a\cos(\Omega t)$. This dissipated energy map was the result of the experimental energy characterisation performed in Ref. [15]. The time series needed for training the neural network were obtained by acquiring sensor measurements. In particular, from the accelerometers we obtain the signal associated with the motion imposed by the shaker, while from the load cells we obtain the force exchanged at the fluid-tank interface. Integrating the acceleration signal yields the velocity signal shown in Figs. 3(a) and 3(b), which is used as input to the model to be identified. Subtracting the inertial force of the fluid from the force measured by the load cells (the sum of the forces measured by the two cells) yields the sloshing force shown in Figs. 3(c) and 3(d), which is the output of the model. These time series are 480 s long with a sample frequency of 0.77 kHz. This sampling rate is the result of a down-sampling process of the original signal, aimed at reducing the length of the time histories in order to facilitate the training phase.

C. Training of neural-network-based ROM

In order to identify a nonlinear reduced order model for vertical sloshing it was decided to exploit an external dynamics strategy, that is, by far, the most widely used approach for modelling and identifying nonlinear dynamical

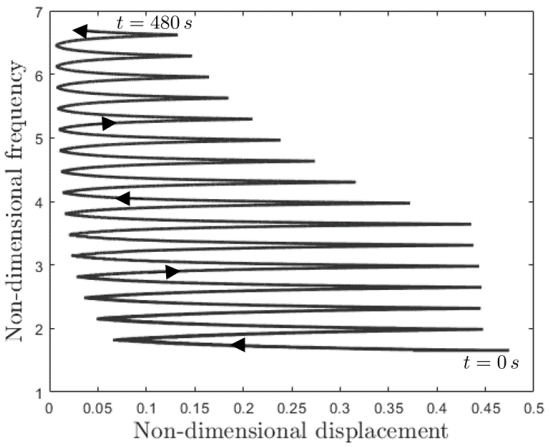

(a) Path of the pseudo-harmonic experimental test

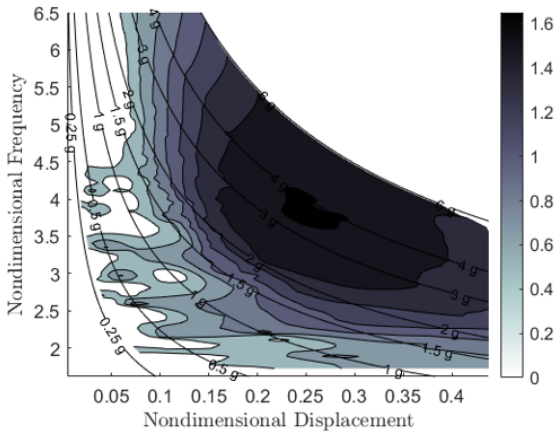

(b) Dissipated energy map

Fig. 2 Path of the pseudo-harmonic experimental test and dissipated energy characterisation

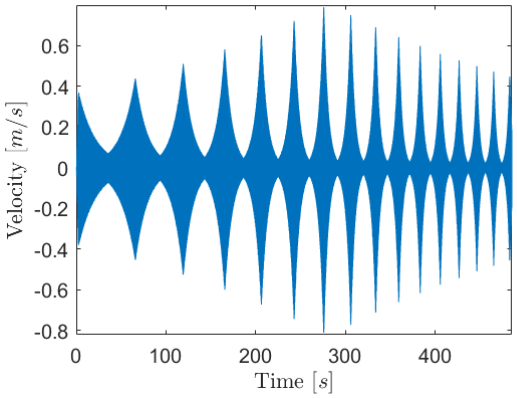

(a) Velocity imposed on the tank

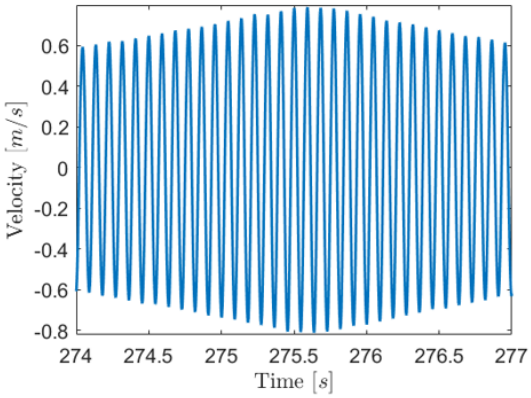

(b) Zoom in Velocity

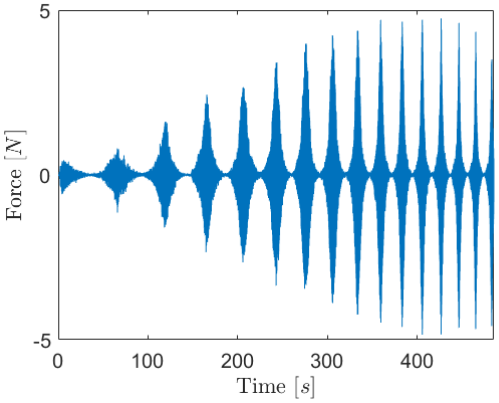

(c) Sloshing force

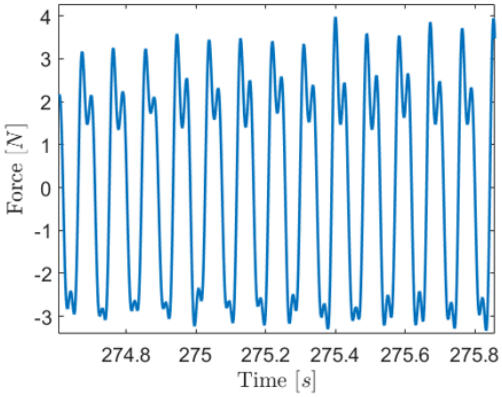

(d) Zoom in sloshing force

Fig. 3 Input-Output time histories for data-driven ROM identification

systems. It is based on a nonlinear input/output model. The name "external dynamics" comes from the fact that the nonlinear dynamic model can be uniquely divided into two parts: a nonlinear static approximator and an external dynamic filter bank. The filters are chosen as simple time delays, while the approximator is chosen as a neural network. A model of this kind is usually called a time delay neural network (TDNN). A nonlinear dynamic model can be used in two configurations: for prediction and for simulation. A prerequisite for prediction is that the process output is measured during operation. In contrast, simulation means that the model simulates only the future outputs based on past process inputs. Therefore, simulation does not require measurements of the process output during operation. The one-step prediction configuration is called a series-parallel model, while the simulation configuration is called a parallel model. The one-step prediction is purely feedforward, while the simulation is recurrent. In this work, it is assumed that the goal of the model is to perform a simulation, that is, it is used in a parallel configuration. This is a much more difficult task than a one-step prediction, since it involves feedback. It is worth noting that a model used in a parallel configuration does not necessarily need to be trained in a parallel configuration. The recommended procedure is to first train a feedforward model and possibly use it as initial model for subsequent optimization (training) of the recurrent model (Ref. [26]). Among the wide variety of NN architectures, a NARX Network in a parrallel configuration has been considered, in which the estimated output is fed back into the network input port (see Fig. 4). It consists of 1 hidden layer with 10 neurons and 1 output layer. Moreover, 2 tapped delay lines are considered for the input and for the output. Hyperbolic tangent functions are employed as activation functions in all nodes of the hidden layer, whereas the output layer is made up with a simple linear function. The *velocity-force* input-output data obtained with the pseudo-harmonic

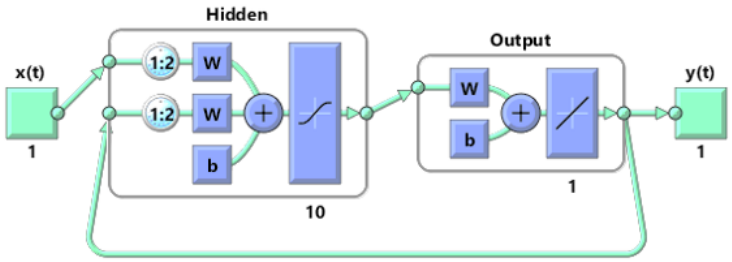

Fig. 4 Neural network architecture

experimental test has been used for the training of the network. In particular, the algorithm used for the training consists of *Levenberg-Marquardt* backpropagation implemented in Matlab® through the *trainlm* function with a fixed number of epochs equal to 500, in which the mean-squared error performance is observed to converge to a constant value, thus guaranteeing the convergence of the network (Ref. [24]). The network was first trained in a feedforward configuration (series-parallel) and then used as the initial model for the recurrent model re-training procedure.

The trained network was then converted into a Simulink® block (using the Matlab function *gensim*) to simulate it and obtain predictions for the output. Figure 5 shows the sloshing force (in red) that the network predicts when it is excited at a velocity equal to that used for the identification (see Figs. 3(a) and 3(b)) compared to the force (in blue) used for the identification process (see Figs. 3(c) and 3(d)). From the comparison figure, it can be seen that the identified network is able to accurately reproduce the nonlinear behavior of the sloshing force.

IV. Sloshing beam response (closed-loop)

In this section, we present the experimental strategy used to validate the reduced-order model identified in the previous section. In particular, in Sec. IV.A we consider a free response problem where the tank presented in Sec. III.A is mounted at the free end of a cantilever beam (experimental sloshing beam model). On the other hand, in Sec. IV.B, we integrate the identified neural network into a closed-loop simulation model that represents the same interaction between sloshing and structure as in the sloshing beam experiment. Finally, validation is performed by comparing the free response results obtained with the experimental and the numerical model.

A. Experimental test case of the sloshing beam

The tank presented in the previous section, which was used to generate the data for the identification of the reduced order model, is placed at the end of a cantilever beam to obtain a new experimental configuration to study the interaction

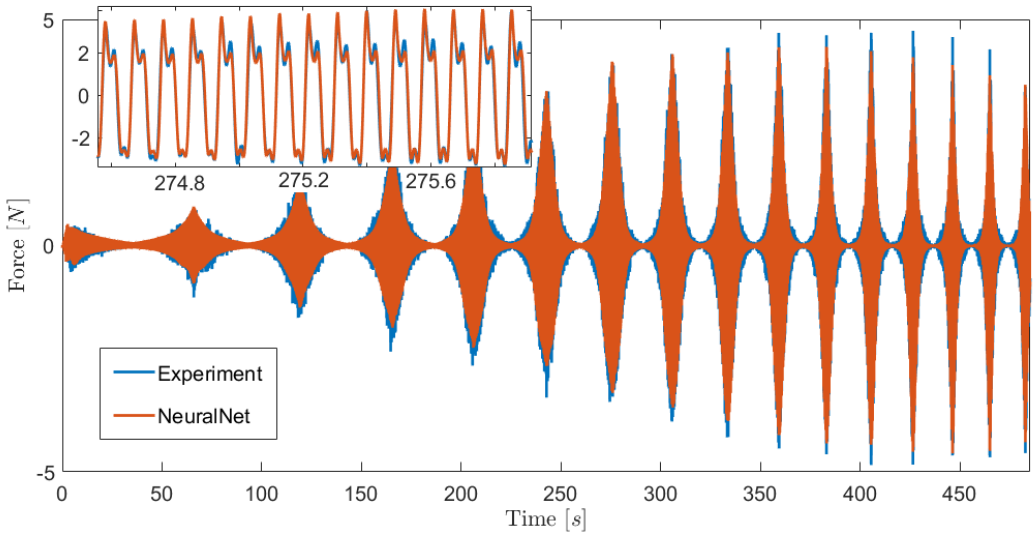

Fig. 5 Comparison between the output predicted by the identified neural network and the experimental time history of the force used for the training

between fluid (liquid stowed in the box) and structure (beam). The two systems (sloshing and beam) interface with each other, defining a *closed-loop* problem, through the motion imposed by the structure and the load returned by the liquid impacts inside the tank. These two actions are measured by accelerometers and load cell sensors, arranged appropriately on the experimental system, shown in Fig. 6. The beam is 74 cm long, 10 cm large, 1 cm thick. Two different configurations are considered in this analysis: the frozen configuration, in which the liquid is replaced by an equivalent not-sloshing mass, and the sloshing case where the liquid is free to slosh and impact the walls of the box. Table 1 shows the main modal quantities of the first three modes of vibration of the cantilever beam (in the configuration

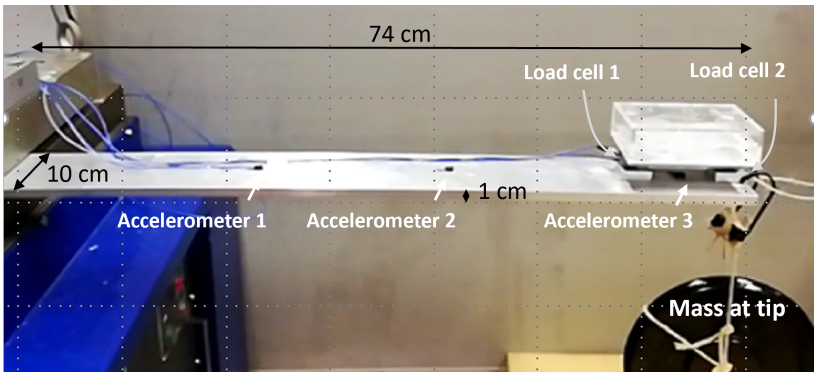

Fig. 6 Layout of the experimental FSI problem

with frozen liquid at the free end). In particular, the experimental natural frequencies are listed, as well as the numerical frequencies derived by a structural updating process. In addition, the table also shows the experimental modal damping coefficients. The modal masses of the beam are also listed based on the numerical model obtained with the structural updating process.

The experimental setup studied is used to obtain experimental reference data that can be used to validate the identified reduced-order model. Similarly to Refs. [11], a free-response problem was considered in this work, where an initial displacement is assigned to the free end of the beam. The release of the beam tip gives rise to the dynamics of the sloshing beam. A mass of 7 kg was used to provide an initial vertical displacement of the beam tip of 1.46 cm. Figure 7 shows the time trends of the free acceleration response signals measured by the accelerometers for the frozen case in Fig. 7(a) and the sloshing case in Fig. 7(b)). The impacts of the liquid with the ceiling of the tank, which occur in the initial

Mode	experimental		numerical	
	f_n [Hz]	ζ_n [%]	f_n [Hz]	m_n [kg]
1	10.87	0.32	10.87	0.8956
2	79.06	0.90	78.31	1.0692
3	223.15	1.76	226.5	0.9655

Table 1 Experimental and numerical natural frequencies f_n, modal damping coefficients ζ_n and modal masses m_n of the cantilever beam with frozen liquid at the free end.

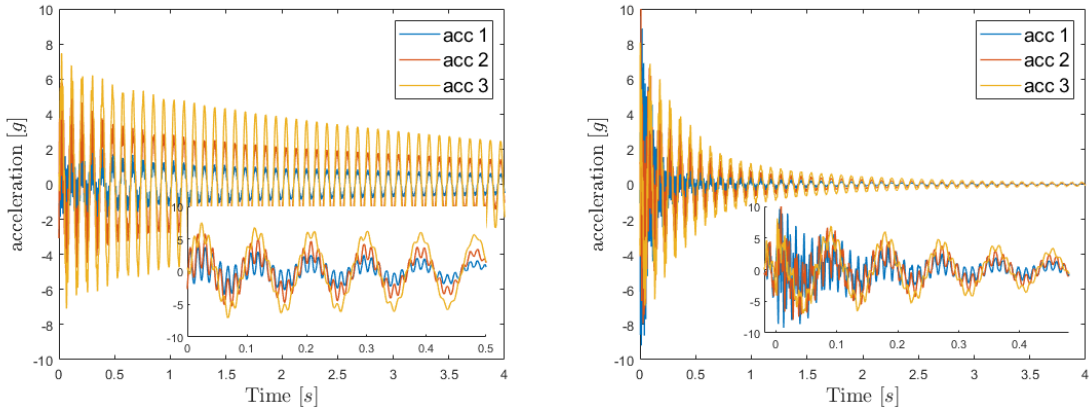

(a) Frozen case (b) Sloshing case

Fig. 7 Comparison between acceleration signals measured by the sensors in the case where the liquid is considered as frozen (a) and in the case where it is free to move (sloshing) (b).

stages of the response, lead to considerable dissipation of energy, resulting in more damped responses than in the frozen case.

By applying the modal filter technique (see Ref. [27]) to the experimental signals measured by the accelerometers, the modal accelerations of the cantilever beam are obtained, by obtaining a separation of the modal contents of the responses. The comparison of the modal accelerations of the frozen case with those of the case where the slosh dynamics is present is shown in Fig. 8.

B. Simulation environment and results

The neural network identified in section III.C is experimentally validated using the free response data obtained with the experimental set-up presented in section IV.A. For this purpose, a simulation model was built in Simulink®, representing the cantilever beam experiment with the addition of the tank with sloshing liquid (see Fig. 9). Figure 9(a) shows the FSI simulation model. The block *structure* contains the modal description of the cantilever beam, while the block *sloshing* (shown in detail in Fig. 9(b)) include the network architecture. It provides the forces returned by the identified neural network-based ROM when it receives as input a given motion of the beam. Note that before and after the network block, gains are required to convert signals from a modal to a point description and vice versa. The point of interest is exactly the one corresponding to the center of the tank, since it is assumed that the sloshing forces act on this point. The two blocks of the closed-loop system interface with each other through modal velocities of the beam and modal loads representing the sloshing forces predicted by the ROM (which in turn go on to affect the structural dynamics creating a fluid-structure interaction problem). The simulation model presented here implements precisely Eq. 2, in which the sloshing forces $\psi_n(x_T)\,\Delta f_{S_z}$ are the loads predicted by the neural network, following the history of the elastic velocity $\sum_m \psi_m(x_T)\dot{q}_m(t)$ evaluated at the tank position x_T. The identified neural network, coupled with the structural dynamics, was used to replicate the same free response of the experimental layout in Sec. IV.A. Figure 10(a)

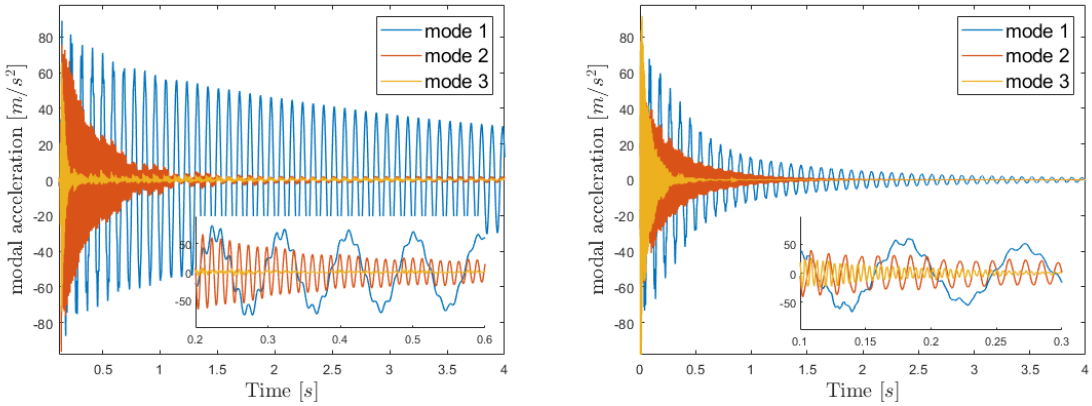

(a) Frozen case

(b) Sloshing case

Fig. 8 Comparison between modal accelerations of frozen (a) and sloshing (b) cases.

shows the predicted numerical acceleration at the centre of tank x_T compared with that obtained by the corresponding experiment. On the other hand, Fig. 10(b) shows the comparison of time histories (numerical and experimental) of the interface forces exchanged between the structure and the tank. It can be noticed that the curves are practically superimposed for both acceleration at tank location and interface force. Figure 11 shows instead the comparison of the instantaneous damping ratio associated to the first mode of vibration. Once the dynamics of the first mode of vibration has been isolated for both experiment and numerical simulation, the instantaneous damping is derived from its envelope by logarithmic decay. Since the envelope decreases monotonically, we can reparametrize the damping as a function of the vertical acceleration of the tank due to the first mode of vibration. Except for the very initial transient (higher accelerations) the neural-network-based ROM looks to provide perfect superimposition in the prediction of the nonlinear damping induced by slosh dynamics.

V. conclusions

In this paper, data-driven nonlinear system identification techniques were exploited to identify a neural network-based reduced order model to describe vertical sloshing. The neural network was trained directly with experimental data. Specifically, an experimental set-up with a box-shaped tank filled halfway with water and placed on an electromechanical shaker was considered for data generation. In this configuration, the vertical sloshing was considered as an isolated system that receives as input an externally imposed motion and returns as output a force arising due to the relative motion of the fluid with respect to the tank and possible impacts of the liquid with the rigid walls of the tank. The motion is generated by the shaker, which is capable of producing intense seismic excitations that can trigger violent sloshing phenomena. The time series required for training the neural network were obtained by acquiring measurements from the sensors. In particular, the system is equipped with accelerometers, to measure the signal associated with the movement imposed by the shaker, and with load cells, to measure the force exchanged at the shaker-tank interface. The experimental test chosen for data generation consisted of a very long pseudo-harmonic excitation cleverly covering the amplitude-frequency range (parameters that are likely to be the most important for characterising the dissipation induced by sloshing). The velocity signal and sloshing force (obtained by subtracting the inertial force of the fluid from the force measured by the load cells) acquired during the pseudo-harmonic test were used respectively as input and output data for the training phase of the network. From the variety of network architectures, a NARX network in a parallel configuration (suitable for simulation purposes) was selected, where the estimated output is returned to the input port of the network. Based on the same velocity signal that was used to train the network, it was able to predict the sloshing force with acceptable accuracy.

In the second part of the paper, we moved from an open-loop logic (sloshing as isolated system) to a closed-loop logic, where the sloshing dynamics interacts with the structural dynamics of a cantilever beam. This transition was used to understand how the identified model would behave in a more complex problem, such as one where it is excited by the elastic displacements of a vibrating beam. So, a new experimental set-up was first designed, in which the tank used to

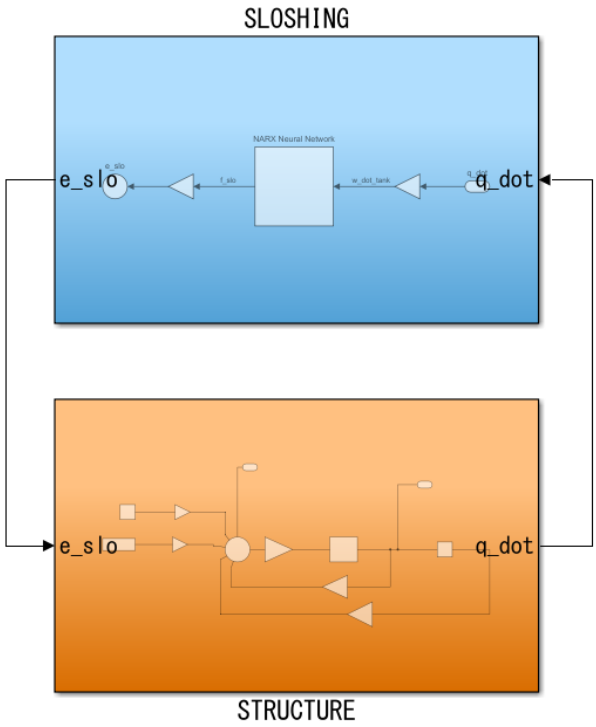

(a) FSI model plant

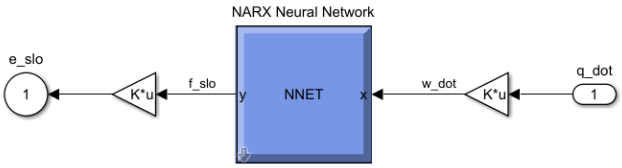

(b) Neural network plant

Fig. 9 Simulink® model representing the sloshing beam experiment

generate the training data was mounted above the free end of a cantilever beam. By using a trigger system at the end of the beam, it was possible to perform a free response analysis from which we collected data over time (both for slosh dynamics and frozen liquid mass). The results of the experimental free response were compared with those obtained by simulating an equivalent virtual model in which the identified reduced-order model is integrated to account for the effects of vertical sloshing. The comparisons showed that the time histories of the acceleration at the end of the beam and the force exchanged at the interface between the tank and the structure are very similar and overlap especially in the first transient of the response. The same is true for the damping characteristic, which was estimated directly from the time trend of the first mode of vibration.

Nonetheless, the identified model works properly because the closed system into which it has been integrated is characterised by having only one dominant oscillatory characteristic. If, on the other hand, the identified network were to interface with a system having more than one dominant harmonic in the interest frequency range, the results might not be as good. The reason lies in the nature of the signal by which the identification was made. Indeed, a pseudo-harmonic test does not allow to obtain signals with which the network can detect more complex dynamics (multi-harmonics). However, this identification technique provides a ROM able to predict the sloshing forces when the structure (*e.g.* an aeroelastic wing) operates close to the stability margin with a main harmonic as in Ref. [28]. Nevertheless, future developments will involve a new identification process that uses experimental data from stochastic tests to train a model capable of capturing multi-harmonic effects.

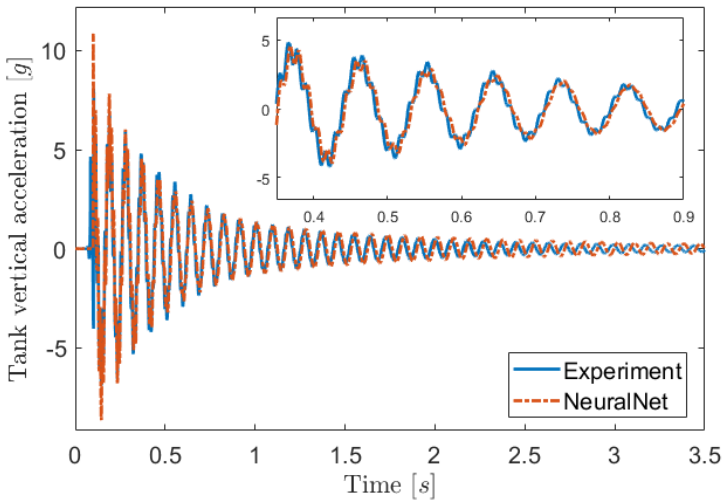

(a) Acceleration at the tank location

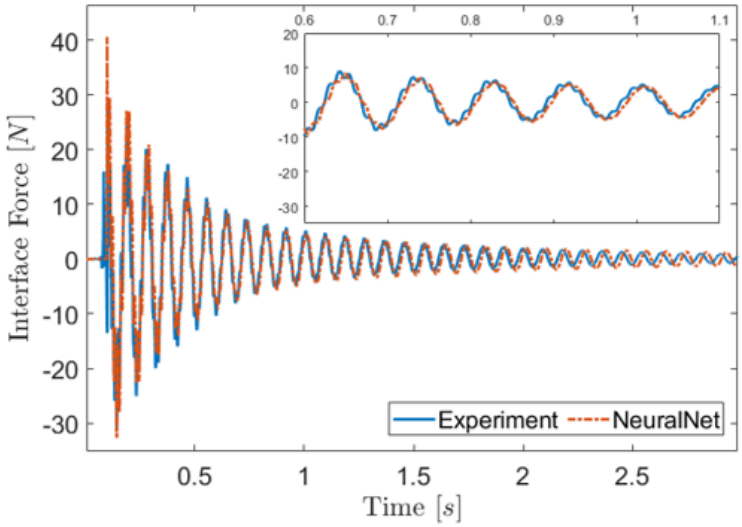

(b) Interface force

Fig. 10 Comparison between the vertical acceleration of the tank and interface forces predicted by the simulation and those obtained by experiments.

Acknowledgments

This paper has been supported by SLOWD project. The SLOWD project has received funding from the European Union's Horizon 2020 research and innovation programme under grant agreement No 815044.

References

[1] Gambioli, F., Chamos, A., Jones, S., Guthrie, P., Webb, J., Levenhagen, J., Behruzi, P., Mastroddi, F., Malan, A., Longshaw, S., Cooper, J., Gonzalez, L., and Marrone, S., "Sloshing Wing Dynamics -Project Overview Sloshing Wing Dynamics – Project Overview," *Proceedings of 8th Transport Research Arena TRA*, 2020.

[2] Graham, E., and Rodriquez, A. M., "The Characteristics of Fuel Motion which Affect Airplane Dynamics," Tech. rep., Douglas Aircraft Co. inc., Defense Technical Information Center, 1951.

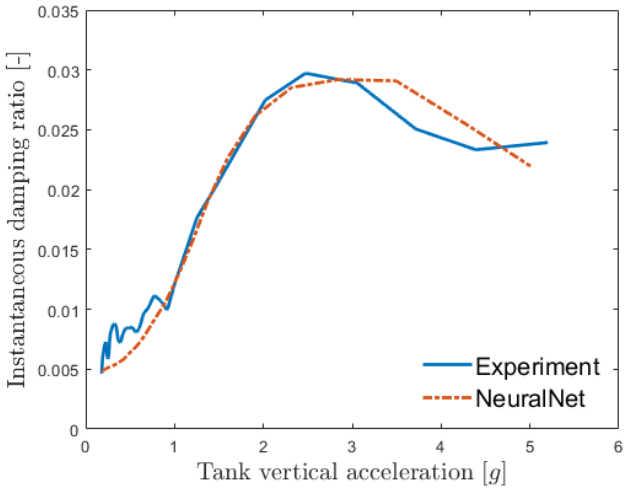

Fig. 11 Instantaneous damping ratio of the first mode of vibration as a function of the acceleration amplitude.

[3] Abramson, H. N., "The dynamic behaviour of liquids in moving containers with applications to space vehicle technology," *Natl. Aeronaut. Sp. Adm.*, 1966, p. 464.

[4] Ibrahim, R. A., "Assessment of breaking waves and liquid sloshing impact," *Nonlinear Dynamics*, Vol. 100, No. 3, 2020, pp. 1837–1925.

[5] Saltari, F., Traini, A., Gambioli, F., and Mastroddi, F., "A linearized reduced-order model approach for sloshing to be used for aerospace design," *Aerospace Science and Technology*, Vol. 108, 2021, p. 106369.

[6] Firouz-Abadi, R. D., Zarifian, P., and Haddadpour, H., "Effect of Fuel Sloshing in the External Tank on the Flutter of Subsonic Wings," *Journal of Aerospace Engineering*, Vol. 27, No. 5, 2014, p. 04014021.

[7] Farhat, C., Chiu, E. K.-y., Amsallem, D., Schotté, J.-S., and Ohayon, R., "Modeling of Fuel Sloshing and its Physical Effects on Flutter," *AIAA Journal*, Vol. 51, No. 9, 2013, pp. 2252–2265.

[8] Pizzoli, M., "Investigation of Sloshing Effects on Flexible Aircraft Stability and Response," *Aerotecnica Missili e Spazio*, Vol. 99, 2020, p. 297–308.

[9] Benjamin, T. B., Ursell, F. J., and Taylor, G. I., "The stability of the plane free surface of a liquid in vertical periodic motion," *Proceedings of the Royal Society of London. Series A. Mathematical and Physical Sciences*, Vol. 225, No. 1163, 1954, pp. 505–515.

[10] Douady, S., "Experimental study of the Faraday instability," *Journal of Fluid Mechanics*, Vol. 221, 1990, p. 383–409.

[11] Gambioli, F., Usach, R. A., Wilson, T., and Behruzi, P., "Experimental Evaluation of Fuel Sloshing Effects on wing dynamics," *18th Int. Forum Aeroelasticity Struct. Dyn. IFASD 2019*, 2019.

[12] Titurus, B., Cooper, J. E., Saltari, F., Mastroddi, F., and Gambioli, F., "Analysis of a Sloshing Beam Experiment," *International Forum on Aeroelasticity and Structural Dynamics. Savannah, Georgia, USA*, Vol. 139, 2019.

[13] Coppotelli, G., Franceschini, G., Titirus, B., and Cooper, J. E., "Oma Experimental Identification od the Damping Properties of a Sloshing System," *Proceedings of Conference on Noise and Vibration ISMA 2020*, Vol. Virtual Event Paper, september 2020.

[14] Coppotelli, G., Franceschini, G., Mastroddi, F., and Saltari, F., "Experimental Investigation on the damping mechanism in sloshing structures," *AIAA Scitech Forum*, Vol. N.6 2021-1388 Virtual Event Paper, January 2021, pp. 11–15 & 19–21.

[15] Saltari, F., Pizzoli, M., Coppotelli, G., Gambioli, F., Cooper, J. E., and Mastroddi, F., "Experimental characterisation of sloshing tank dissipative behaviour in vertical harmonic excitation," submitted to *Journal of fluids and structures*, 2021.

[16] Constantin, L., De Courcy, J., Titurus, B., Rendall, T., and Cooper, J., "Analysis of damping from vertical sloshing in a SDOF system," *Mechanical Systems and Signal Processing*, Vol. 152, 2021, p. 107452.

[17] Nastran, M., *Dynamic Analysis User's Guide*, 2012.

[18] Eugeni, M., Saltari, F., and Mastroddi, F., "Structural damping models for passive aeroelastic control," *Aerospace Science and Technology*, Vol. 118, 2021, p. 107011.

[19] Balmes, E., and Leclère, J., *Viscoelastic Vibration Toolbox, User's Guide*, 2017.

[20] De Courcy, J. J., Constantin, L., Titurus, B., Rendall, T., and Cooper, J. E., "Gust Loads Alleviation Using Sloshing Fuel," *AIAA Scitech 2021 Forum*, 2021.

[21] Pizzoli, M., Saltari, F., Mastroddi, F., Martinez-Carrascal, J., and González-Gutiérrez, L. M., "Nonlinear reduced-order model for vertical sloshing by employing neural networks," *Nonlinear dynamics*, 2021.

[22] Ahn, Y., Kim, Y., and Kim, S.-Y., "Database of model-scale sloshing experiment for LNG tank and application of artificial neural network for sloshing load prediction," *Marine Structures*, Vol. 66, 2019, pp. 66–82.

[23] Ahn, Y., and Kim, Y., "Data mining in sloshing experiment database and application of neural network for extreme load prediction," *Marine Structures*, Vol. 80, 2021, p. 103074.

[24] Beale, M. H., Hagan, M. T., and Demuth, H. B., *Deep Learning Toolbox*, Mathworks, 2020.

[25] Martínez-Carrascal, J., and González-Gutiérrez, L., "Experimental study of the liquid damping effects on a SDOF vertical sloshing tank," *Journal of Fluids and Structures - Submitted*, 2020.

[26] Nelles, O., *Nonlinear system identification, from classical approaches to neural networks, fuzzy models, and gaussian processes*, 2nd ed., Springer, 2021.

[27] Meirovitch, L., and Baruh, H., "Implementation of Modal Filters for control of structures," *Journal of Guidance, Control, and Dynamics*, Vol. 8, 1985, p. 707–716.

[28] Saltari, F., Pizzoli, M., Mastroddi, F., Gambioli, F., and Jetzschmann, C., "Nonlinear sloshing integrated aeroelastic analyses of a research wing prototype," *AIAA Scitech 2022 Forum*, 2022.